



UNIVERSITÀ
DEGLI STUDI
DI PADOVA

Università degli Studi di Padova

Padua Research Archive - Institutional Repository

Space tethers: parameters reconstructions and tests

Original Citation:

Availability:

This version is available at: 11577/3394817 since: 2022-01-31T16:53:20Z

Publisher:

Published version:

DOI: 10.1109/MetroAeroSpace51421.2021.9511677

Terms of use:

Open Access

This article is made available under terms and conditions applicable to Open Access Guidelines, as described at <http://www.unipd.it/download/file/fid/55401> (Italian only)

(Article begins on next page)

Space tethers: parameters reconstructions and tests

Alice Brunello

*Center of Studies and Activities for Space
"Giuseppe Colombo" (CISAS)
University of Padua
Padua 35131, Italy*
alice.brunello.3@phd.unipd.it

Lorenzo Olivieri

*Center of Studies and Activities for Space
"Giuseppe Colombo" (CISAS)
University of Padua
Padua 35131, Italy*
lorenzo.olivieri@unipd.it

Giulia Sarego

*Center of Studies and Activities for Space
"Giuseppe Colombo" (CISAS)
University of Padua
Padua 35131, Italy*
giulia.sarego@unipd.it

Andrea Valmorbida

*Departement of Industrial Engineering
University of Padua
Padua 35131, Italy*
andrea.valmorbida@unipd.it

Enrico Lungavia

*University of Padua
Padua 35131, Italy*
enrico.lungavia@studenti.unipd.it

Enrico C. Lorenzini

*Departement of Industrial Engineering
University of Padua
Padua 35131, Italy*
enrico.lorenzini@unipd.it

Abstract — In the last several years, the need for an alternative to chemical propulsive systems for low-orbit satellite deorbiting has become increasingly evident; a Tethered System can provide adequate thrust or drag without the complications of combustions and with a minimal impact on the environment. In this context, the authors are part of a team that is studying various tether applications and building a prototype of an electrodynamic tether system. The goal of this paper is to characterize tether materials in order to find valid solutions for future space tether missions. Mission requirements (e.g., the survivability to hypervelocity impacts and the capability to damp oscillations in electrodynamic tethers) influence the choice of tether parameters such as cross section geometry (round wires or tapes), materials, length, and cross section sizes. The determination of the elastic characteristics and damping coefficients is carried out through a campaign of experiments conducted with both direct stress/strain measurements and the laboratory facility SPACecRraft Testbed for Autonomous proximity operations experimentS (SPARTANS) on a low friction table at the University of Padova. In the latter case, the stiffness and damping of a flexible line were verified by applying different tensile load profiles and then measuring the tether-line dynamic response in terms of tension spike amplitude, oscillation decay, and estimation of the damping coefficient.

Keywords—Space tethers, elastic parameters estimation, damping coefficient estimation

I. INTRODUCTION

The project of a tethered vehicle can lead to a new technological solution for generating propulsion in space that is safe and free of contaminants: characteristics that are becoming necessary for the future viability of our Earth and Space. The need for an alternative to chemical propulsive systems for low-orbit satellites has become increasingly evident and an Electrodynamic Tether System (EDT) is able to provide adequate thrust or drag without the complications of combustions and with a minimal impact on the space environment. In this way the purity of the space environment for science payloads will be enhanced, and beneficial operational impacts of reduced propellant exhaust on external systems and optics will be realized. Finally, outfitting a satellite with a tether severs the most critical and constraining

dependency of space systems, i.e., the need for propellant resupply. Consequently, benefits in using Tether Systems are manifolds and its value lies in the fact that they are able to generate clean propulsion in total autonomy by exploiting physical principles: angular momentum conservation, pairing between energy generation and thrust or vice versa between a decrease in orbital energy and production of electrodynamic drag. By releasing satellites from sensitive space environment as the ISS employing inert tethers, the external contamination around that platform is greatly reduced [1,2]; equipping Satellites with an electrodynamic tether [3,4] ensures independence from the storage and use of propellant in orbit. Consequently, the tasks of deorbiting, re-entry and reboost and, in general, passive propulsion can be addressed by a technology that is increasingly mass-efficient as the time in orbit increases when compared to chemical systems. For all these reasons it has become essential to characterize tethers, studying the mechanical characteristics of materials in order to meet mission requirements in term of hypervelocity impact survivability [5] and the ability to damp out tether oscillations [6], in order to find out valid material solutions for future space tether missions. A test campaign was carried out on different materials, using a dedicated test bed to determine tether mechanical properties and verifying them with the SPARTANS low-friction facility of the University of Padova. In particular, the stiffness and damping coefficients of tether samples were verified by applying different tensile loads in slack conditions and then measuring the tether dynamic response in terms of tension spikes, oscillation frequency, and damping.

II. TETHER MATERIALS AND CURRENT RELATED MISSIONS

The materials that we analyzed are those that have been most frequently used in past tethered missions [7] or materials that are currently being considered because of their potential to be applied to future missions in terms of: (a) survivability to hypervelocity impacts, and (b) the ability to damp oscillations, that is particularly important for electrodynamic tether applications.

Space tethers were first proposed in the early 1970s by Giuseppe Colombo and Mario Grossi and the first orbital experiments flew on board the Space Shuttle in the 1990s [8] to demonstrate the feasibility of deploying long tethers and to conduct experiments in space plasma physics.

Space tethers can be inert or conductive and most of those used in the past had circular cross sections. Inert tethers are non-conductive, typically made of Kevlar, Spectra or Nylon,

and in some specific applications they allow momentum to be transferred between objects in space. An interesting current mission concept that could use a Nylon tether is “CUTIE” [9], that consists of a dual Cubesat system for orbital insertion designed for Moon exploration. A future mission using a Spectra Tether can be identified with “Iperdrone.1” which aims to analyze the feasibility of deorbiting a reentry capsule from the ISS using a momentum-exchange tether [10,11]. Electrodynamic tethers can be designed to produce several useful effects by interacting with the orbital environment: instead of carrying propellant, a long conducting tether, coated in part with a thin layer of a low-work function material (to act as a cathode), will produce a propulsive force by taking advantage from the natural space environment (geomagnetic field, ambient plasma and solar radiation). A recent project funded by the European Commission - BETs - [12] analyzed in details the use of electrodynamic tape tethers instead of round tethers due to their higher survivability to space debris impacts and a better electrodynamic performance due to the larger perimeter of the tether cross section for equal tether mass. A multi-national study currently been conducted on the use of tape tethers for deorbiting is the H2020 European project “E.T.PACK” [13]. The materials investigated in our research program, their dimensional characteristics and the related missions are summarized in Table I.

TABLE I. TETHER CHARACTERISTICS INVESTIGATED

<i>Tether characteristics investigated</i>			
<i>Materials</i>	<i>Tether geometry</i>	<i>Cross Section</i>	<i>Related mission</i>
Nylon	Round	0.0707 [mm ²]	CUTIE
Spectra™	Braided	2 [mm] x 1.5 [mm] (elliptical)	Iperdrone
Al-1100	Tape	(0.05 x 25.00) [mm ²]	E.T.PACK
PEEK	Tape	(0.05 x 25.00) [mm ²]	E.T.PACK

III. EXPERIMENTS

The experimental campaign was divided in two phases. First, two simplified setups were employed to determine Young modules and damping coefficients for Aluminum Al-1100 and PEEK tape materials; a second phase was dedicated to the experiments carried out using the SPARTANS facility.

A. Young modulus determination for tapes

The two tapes Young modules were calculated through the measurement of the tape elongations for different loading conditions. For each tape, a three meters long section was hung up and three loads were applied at least three times each; the elongation was measured with an analog indicator with a resolution of 0.01 mm. The two materials stiffness (k) and Young module (E) are reported in Table II; the associated 1- σ uncertainty was calculated through error propagation according to the GUM [14].

TABLE II. MATERIALS STIFFNESS AND YOUNG MODULE FOR THE TWO TAPES

<i>Tether characteristics investigated</i>		
<i>Materials</i>	<i>K [N/m]</i>	<i>E [Gpa]</i>
Al-1100	24734.25 \pm 335.52	59.16 \pm 3.29
PEEK	1810.91 \pm 7.53	4.35 \pm 0.23

While the value for PEEK is consistent with available data [15], the Al-1100 reference Young modulus is 69.0 GPa [16], about 14% larger than the experimental result.

The Aluminum tape was previously employed in the deployment tests reported in [17], resulting in a partial deformation of the sample edge, as reported in Fig. 1. The resulting plastic strain might have reduced the effective area on which the load can act.

Despite this small discrepancy between the experimental result and the literature data, the calculated Young modulus was adopted in the parameters reconstruction, as the same section of the tape was employed in the remainder of the experimental campaign and the detected strain is representative of potential damages during the tether deployment.

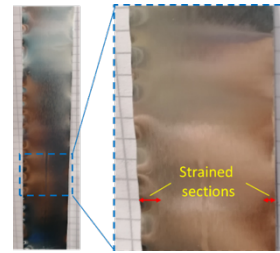


Fig. 1 Test sample (left) and detail (right) with strained sections highlighted

B. Damping coefficient determination for tapes

An experiment with the use of a laser vibrometer was performed to determine the damping coefficient c of Aluminium and Peek tapes. Fig. 2 shows the schematic of the implemented setup.

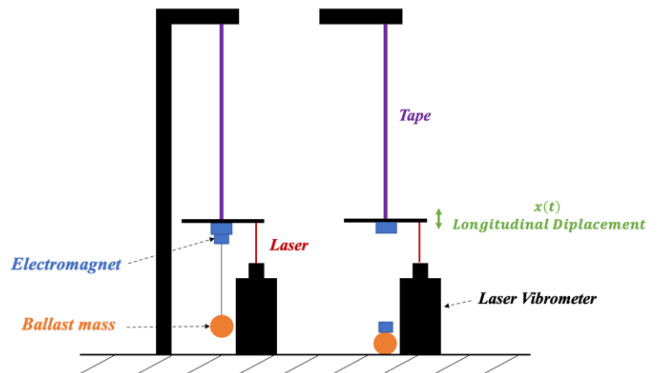


Fig. 2 Experimental setup: the laser vibrometer measures the longitudinal displacements of the plate connected to the lower end of the tape. The oscillation is generated by releasing with a magnet a known mass connected to the plate.

The experiment helped us to determine the logarithmic decrease $\delta(t)$ of the tape material, and consequently the damping coefficient, c . The logarithmic decrement represents the rate at which the amplitude of a free damped vibration decreases. It is defined as the natural logarithm of the ratio of any two successive peak amplitudes and it is found from the time response of the underdamped vibration (Fig. 3).

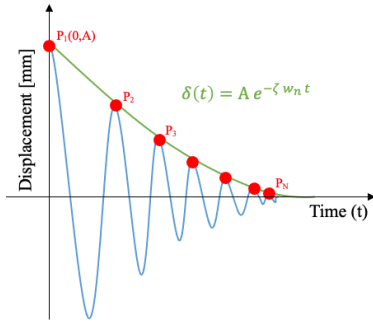


Fig. 3 Illustration of the logarithmic decrement method. The blue line represents the time response of the underdamped vibration. The green line is the envelope of time response peaks and is used to determine the logarithmic decrement function.

A campaign of tests was carried out in order to find the time response of the underdamped vibration for each tape material investigated. Fig. 4 shows an example of time response spectrum for a Peek sample test obtained using DIAdem[®].

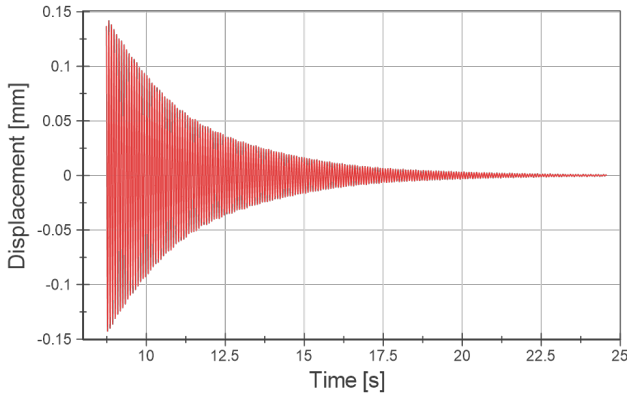


Fig. 4 Time response of a test with PEEK. The signal is filtered and cleaned from contributions from the transverse displacement of the plate, that generates frequencies in planes other than the longitudinal one.

The logarithmic decrement for all tests conducted on Peek material are shown in Fig. 5.

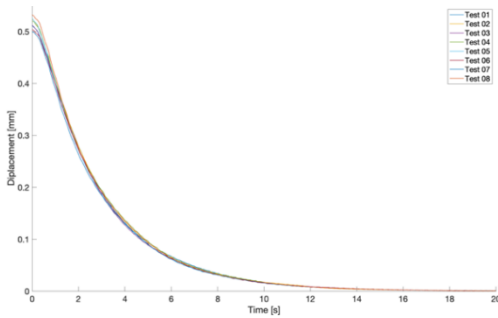


Fig. 5 Logarithmic decrements for all tests conducted on the Peek material. The damping coefficient c was obtained by averaging the individual coefficient c for each test.

Through these analyses, first we computed the damping ratio ζ from the logarithmic decrement $\delta(t)$ ($\delta(t) = Ae^{-\zeta\omega_n t}$, see Fig. 3) and then the average damping coefficient c , for the two tape materials investigated, simply reversing eqn. (1):

$$\zeta = \frac{c}{2\sqrt{k m}} \quad (1)$$

The resulting values are reported in Table III.

TABLE III. DAMPING COEFFICIENT FOR THE TWO TAPES

Tether characteristics investigated	
Materials	Damping Coefficient (c)
Al-1100	48.81 Ns/m
PEEK	0.37 Ns/m

C. SPARTANS facility: experimental setup

The remainder of the experimental campaign was conducted by using the SPARTANS facility in order to estimate both the damping coefficient and the stiffness of the four tether samples listed in Table I in a configuration that mimics the separation phase of E.T.PACK. The SPARTANS facility [18,19,20] consists in a 3×2 m² test table and a module/spacecraft unit. Specifically, the spacecraft unit is composed by a translational module and an attitude module and its motion is tracked by a Motion Capture (MC) system that employs 6 external infrared (IR) cameras and a set of spherical IR markers placed on the unit (Fig. 6, left) [21]. A dedicated Deployer Mechanism Mockup [17] is mounted on the SPARTANS translational module (Fig. 6, right); in this configuration the whole free-floating system has a mass of about 25 kg and three degrees of freedom (two translations on the test table and the rotation around the vertical axis).

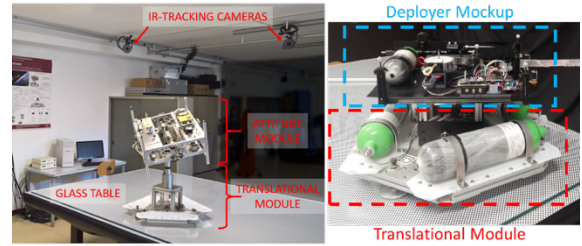


Fig. 6 The SPARTANS facility (left) and the dedicated Deployer Mockup (right).

The free end of the tether is attached to a dedicated structure on one edge of the test table. A load cell is placed between the tether and the fixed structure to measure the magnitude of the transmitted loads (Fig. 7). The whole free-floating system is equipped with a Wi-Fi communication link and an external control station was used to conduct the experiments, collect data and monitor the system.

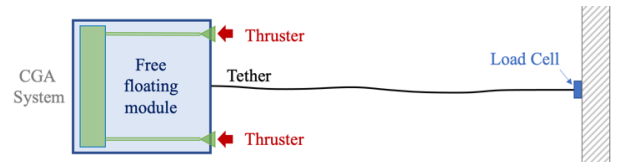


Fig. 7 Experimental setup layout with the free-floating module, the tether line, and the constrained load cell.

Referring to Fig. 7, a tether sample was connected to the translation module and to the fixed load cell; starting from a slack condition (i.e., a distance between the module and the load cell shorter than the line length), the thrusters on board the module were activated and the MC system was used to measure the tether response to an impulsive load or to a constant-force step function. In the first case, the module thrusters were deactivated before the line was fully stretched,

while in the second case the thrusters remained active until the transient phase was completed and the line was in tension.

IV. PARAMETER RECONSTRUCTIONS

With the experimental setup described, the translation module motion was reconstructed and compared to simulations and the tension on the tether was measured with the load cell mounted on the fixed end. The objective was to reconstruct and compare tests with simulations in order to determine or verify the tether mechanical properties. Stiffness and damping coefficients for Spectra and Nylon were determined through an optimization tool and comparisons between the simulated and experimental tether line dynamic responses. For PEEK and Aluminum tapes, parameters obtained from the experiments described in section III were used to match simulations and tests.

A. Simulations: mass-spring-damper equivalent system

A mass-spring-damper equivalent system (Fig. 8) was used to model the behavior of the tether during experiments. Each test was represented with a simple equivalent system modelled in MatlabTM:

$$m\ddot{x} + c\dot{x} + kx = F_{THRUSTERS}(t) + F_{FRICTION}(t) + T_{TETHER}(t) \quad (2)$$

where m is the mass of the translation module of 25 kg, c the tether damping coefficient, and k the material stiffness. $F_{THRUSTERS}(t)$ is the total force produced by the thrusters on board the translation module (each thruster generates a calibrated force of $F_{THRUSTERS}(t)/2$), $F_{FRICTION}(t)$ is the frictional force between the whole free-floating system and the test table, and $T_{TETHER}(t)$ is the resulting tether tension due to the tether weight.

The spring-mass-mode material stiffness is given by $k = \frac{EA}{L}$ where A is the tether cross section area and L the tether length. The elastic modulus is a value readily available in the literature for the material but, because our work consisted in verifying the theoretical value, k became a variable for the simulated system; the value of k for the two tapes was derived from data reported in Table II.

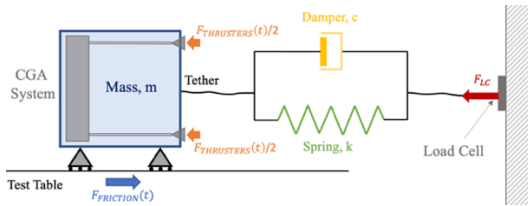


Fig. 8 Mass-spring-damper equivalent system

B. Tether Weight

The weight of the tether can affect the simulation results. For this reason, it was essential to introduce the effect of the weight of the material in the simulations. For our purpose, the catenary load was used to implement the effect of the tether weight on the resulting tether tension (see Fig. 9). The equation of the catenary with two attachment points is shown in the following:

$$T_{tether} = \frac{qL^2}{8\sqrt{\frac{3L(s-L)}{8}}} \quad (3)$$

where $q = \lambda g$, λ is the linear density of the tether material and $g = 9.8 \text{ m/s}^2$; L is the distance between the constraints and s is the catenary length with $s \cong L + 8h^2/(3L)$.

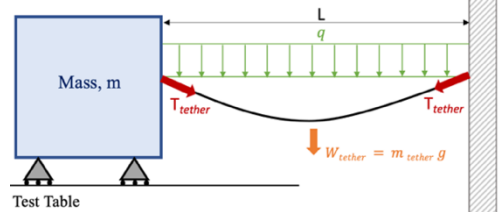


Fig. 9 The catenary scheme used to implement the effect of the tether weight, W_{tether} , on the resulting tether tension, T_{tether}

C. Optimization for Nylon and SPECTRATM

An optimization tool was used to determine the mechanical characteristic of Nylon and SPECTRATM. Those materials, due to inherent characteristics (i.e. differential elongation due to the braided cross section), require dedicated considerations and a particular setup. This means an in-depth study and, we would like to say, that is our intention to go into more details of the behavior of those materials in the future. Unlike what was done for All-1100 and PEEK (Young modulus and damping coefficient determined experimentally and described in section III), to date they have been studied from a numerical point of view, which will certainly be a good starting point for subsequent analyses. The parameters k and c that characterize the mathematical model of the mass-spring-dumper dynamic system were estimated from the measured/estimated data, which are the tether length, $l_{tether}(t)$, derived from the MC system output, and the force measured by the load cell, $F_{LC}(t)$, given the known input $F_{THRUSTERS}(t)$. Specifically, the model of the system is estimated by tuning its unknown parameters k and c such that the model output is close to the measured output, as depicted in Fig. 10. We used the functions available in the MatlabTM Optimization Toolbox to minimize the Root Mean Square (RMS) discrepancy between the model output and the measured ones.

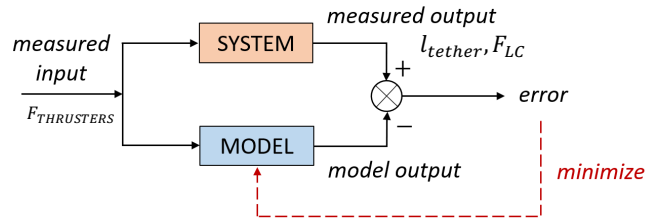


Fig. 10 Block diagram showing the minimization process used to identify the parameters k and c of the mathematical model of the mass-spring-dumper system.

V. RESULTS

In this section, results related to the four materials investigated: Nylon, SpectraTM, Al-1100, Peek.

A. Nylon tether

The proposed numerical method was first used to test the mechanical characteristic of a 1.5 m long polyamide line (Nylon) with a diameter of 0.3 mm and with an average theoretical stiffness of 129 N/m. Results for the polyamide line are reported in Fig. 11 and Fig.12. Two different thrust levels, 0.38 N and 0.62 N, where utilized in the test. To match

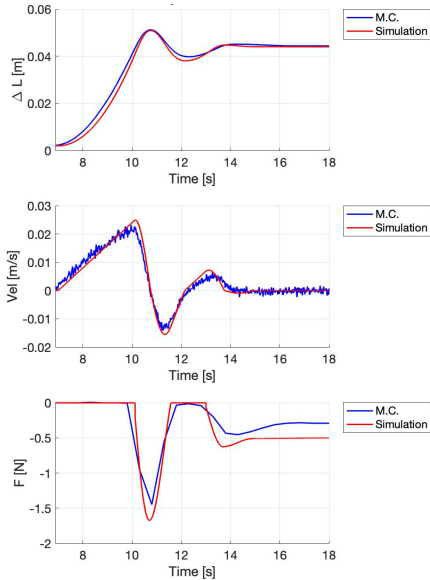


Fig. 11 Polyamide line mechanical characteristics verification with low thrust level ($F_T = 0.38\text{ N}$): comparison of experimental data (solid blue lines) with results from simulations (red lines). From top to bottom: S-DM translation, S-DM velocity, and tether tension.

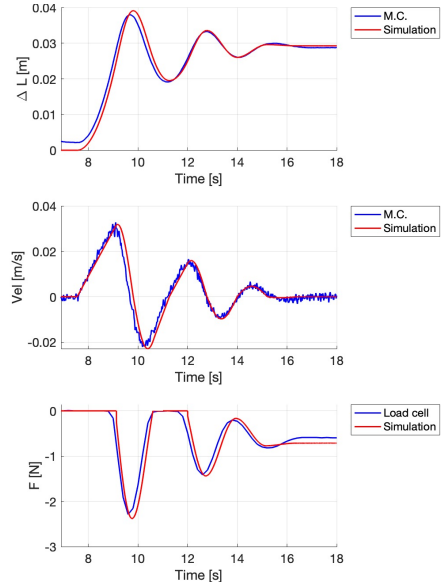


Fig. 12 Polyamide line mechanical characteristics verification with high thrust level ($F_T = 0.62\text{ N}$): comparison of experimental data (solid blue lines) with results from simulations (red lines). From top to bottom: S-DM translation, S-DM velocity, and tether tension.

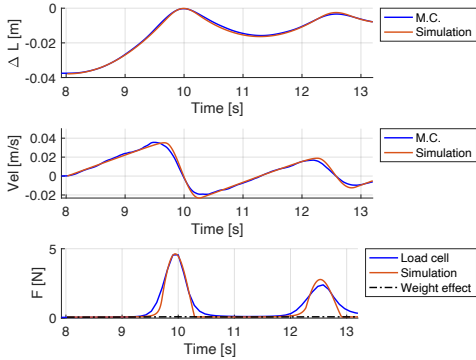


Fig. 13 Spectra™ braided tether mechanical verification with step impulse: comparison of experimental data (solid blue lines) with results from simulations (red lines). From top to bottom: S-DM translation, S-DM velocity, and tether tension.

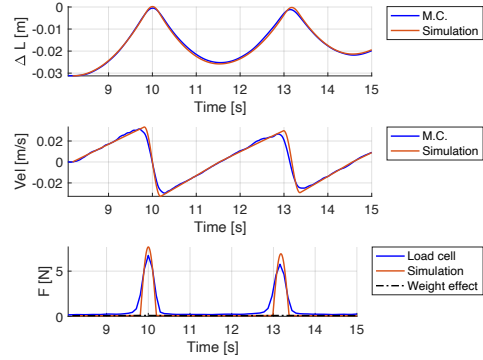


Fig. 14 Peek tether mechanical verification with step impulse: comparison of experimental data (solid blue lines) with results from simulations (red lines). From top to bottom: S-DM translation, S-DM velocity, and tether tension.

simulations with the experimental data, the optimization tool found a damping coefficient of 8 N s/m corresponding to a damping ratio $\zeta = 6.18\%$ and a stiffness of 167.64 N/m . The difference from the average theoretical value of about 30% can be found in the lack of knowledge of the actual Nylon composition. All discrepancies between experiments and simulations are related to the residual friction effects between the translation module and the test table.

B. SPECTRA™ tether

Results for the SPECTRA™ braided tether are reported in Fig. 13. The optimization tool find a a damping coefficient of 35 Ns/m (corresponding to a damping ratio $\zeta = 12.75\%$) and a stiffness of 753.33 N/m . Due to the high value of the damping coefficient the braided structured seems to be more efficient in damping oscillations.

C. PEEK tape

As mentioned before, two experiments were performed to determine the stiffness and the damping coefficient of this material. The experiment helped us to determine the logarithmic decrease of the material $\delta(t)$ and thus the average damping coefficient (c). Results for the 3-m Peek tape are reported in Fig. 14 and were obtained by forcing the

system with a unitary step function. The simulation data are for an average damping coefficient of 0.37 Ns/m . The stiffness ($k = \frac{EA}{L}$) of 1810.91 N/m was obtained using the average value of the Young modulus (E) previously calculated with the experiment described in section III,A. Discrepancies between experiments and simulation are very small; the proposed system is therefore representative for verifying the PEEK tape mechanical parameters and its performance for tethered applications.

D. Aluminium tape

The two experiments previously decribed identified, for a 3-m Aluminum tape, $k = 24734.25\text{ N/m}$ and $c = 48.16\text{ Ns/m}$ ($\zeta = 14\%$). Results for the Aluminum tape are reported in Fig. 15 and were obtained using a unitary step forcing function. In this last case, discrepancies between experiments and simulation are related to the higher stiffness of the investigated sample, that is comparable with the experimental setup equivalent stiffness. In this case, different phenomena are present and the model implemented in the simulations is only partially representative; results shown in Fig. 15 show the best fit of the experimental data.

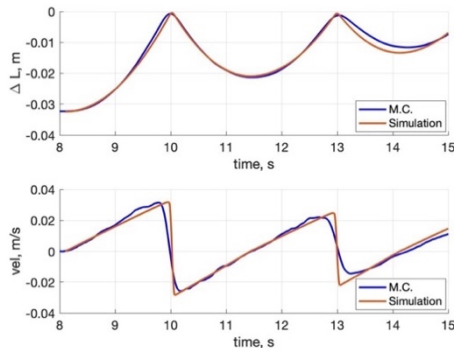


Fig. 15 Aluminum tether mechanical verification with step impulse: comparison of experimental data (solid blue lines) with results from simulations (red lines). From top to bottom: S-DM translation and S-DM velocity.

VI. CONCLUSIONS

This paper presented the parameters reconstruction of space tethers. Four materials were investigated: Nylon, SPECTRA™, Peek and Aluminum. Those materials are the most typical for present and future tethered space missions. Due to lack of knowledge in the Nylon material and the differential elongation related to the braided cross section of SPECTRA™, these materials were numerically investigated through the use of an optimization tool in MATLAB®.

The parameters k and c , that characterize the mathematical model of the mass-spring-damper dynamic system, were estimated by “tuning” them with an optimization tool in order to obtain the dynamic response as close as possible to the one measured with the experiment conducted with SPARTANS facility. Parameters for PEEK and Aluminum were investigated by using two experimental setups, allowing: a) the determination of Young modulus through the measurement of the tape elongations for different loading conditions and b) the determination of the damping coefficient through the use of a laser vibrometer. All the parameters were then used to compare the experimental data given by the SPARTANS facility with the simulation of the mass-spring-damper equivalent system. All the calculated parameters, summarized in Table IV, allow to obtain dynamic responses very similar to those estimated with the use of the SPARTANS Facility. It is our plan to proceed with experimental analysis on Nylon and SPECTRA™ to confirm the simulated parameters.

In conclusion, we proved that the main parameters of tether materials can be verified in the operational setup provided by the SPARTANS facility. Experimental campaigns investigating the use of tethers in a relevant environment provided by SPARTANS can therefore include tether materials verification without the need for additional setups.

TABLE IV. SPACE TETHER PARAMETER: SUMMARY

<i>Space tether parameters</i>		
<i>Materials</i>	<i>Stiffness</i>	<i>Damping coefficient</i>
Nylon	167.64 N/m	8 Ns/m
Spectra™	753 N/m	35 Ns/m
Al-1100	24734.25 N/m	48.16 Ns/m
PEEK	1810.91 N/m	0.37 Ns/m

ACKNOWLEDGMENT

The authors wish to thank Davide Vertuani and Mirco Bartolomei for their support in the development of the

experimental setup. This work was supported by the European Union’s H2020 Research and Innovation Program under Grant Agreement no. 828902 (E.T.PACK Project).

REFERENCES

- [1] S. Ianneli, M. Albano, M. Di Clemente, A. Gabrielli, S. Cantoni, M. De Stefano Fumo, R. Votta, A. Fedele, R. Gardi, M. Cardi, F. Corradino, F. Carrai, F. Carubia, A. Brunello, E. Lorenzini, D. Zuin, S. La Luna, M. Valli, A. Zamprota, F. Punzo, “On orbit and re-entry services performed by Space Drones”, FAR2019, Monopoli (Italy), 2019.
- [2] <https://www.cira.it/it/comunicazione/news/il-programma-iperdrone-presentato-per-i-20-anni-della-iss>
- [3] G. Sarego, L. Olivieri, A. Valmorbida, A. Brunello, E. C. Lorenzini, L. Tarabini Castellani, E. Ugoiti, A. Ortega, G. Borderes-Botta And G. Sanchez-Arriaga, “Deployment Requirements For Deorbiting Electrodynamic Tether Technology”, Ceas Aerospace Europe Conference, Bordeaux, 2020.
- [4] Fet Open Project, Electrodynamic Tether Technology For Passive Consumable-Less Deorbit Kit (E.T.Pack), No. 828902, 1/3/2019-31/5/2022, <https://etpack.eu/>
- [5] A. Francesconi, C. Giacomuzzo, F. Branz, E.C. Lorenzini “Survivability to hypervelocity impacts of electrodynamic tape tethers for deorbiting spacecraft in LEO”, 6th European conference on space debris, Darmstadt (Germany), April 2013.
- [6] R. Mantellato, M. Pertile, G. Colombatti, A. Valmorbida, E.C. Lorenzini, “Two-bar model for free vibrations damping of space tethers by means of spring-dashpot devices”, CEAS Space Journal. 6. 133-143. 10.1007/s12567-014-0065-x, 2014.
- [7] M. L. Cosmo, E.C. Lorenzini, “Tethers In Space Handbook”, Resource Online: <https://www.nasa.gov/centers/marshall/pdf/337451main>
- [8] Dobrowolny, M., & Stone, N. H. (1994). A technical overview of TSS-1: the first tethered-satellite system mission. *Il Nuovo Cimento C*, 17(1), 1-12.
- [9] C. Bettanini, E.C. Lorenzini, G. Colombatti, A. Aboudan, M. Massironi, “CUTIE: A cubesats tether-inserted mission for moon exploration”, *Acta Astronautica*, Vol. 152, Nov. 2018, 580-587, DOI: 10.1016/j.actaastro.2018.09.005, Elsevier Ltd, ISSN: 00945765, 2018
- [10] A. Brunello, A. Valmorbida, E.C. Lorenzini, S. Cantoni, M. De Stefano Fumo, A. Fedele, R. Gardi, R. Votta, “Deorbiting small satellites from the ISS using a tether system”, *CEAS Space J* 2020, <https://doi.org/10.1007/s12567-020-00337-1>
- [11] A. Brunello, A. Valmorbida, E. C. Lorenzini, A. Fedele, M. De Stefano Fumo, R. Votta, “Tethered Satellite controlled re-entry dynamics from the International Space Station”, *IEEE MetroAeroSpace*, Pisa, June 2020.
- [12] J. R. Sanmartin Losada et al. “BETS: Propellant less deorbiting of space debris by bare electrodynamic tethers”, ISBN 978-92-79-22207-8.
- [13] G. Sánchez-Arriaga, S. Naghdi, K. Wätzig, J. Schilm, E.C. Lorenzini, M. Tajmar, E. Ugoiti, L. Tarabini Castellani, J.F. Plaza and A. Post, “The E.T.PACK project: Towards a fully passive and consumable-less deorbit kit based on low-work-function tether technology”. *Acta Astronautica*, Vol. 177, December 2020, pp. 821-827.
- [14] BIPM, IEC, IFCC, ILAC, ISO, IUPAC, IUPAP, OIML. *Evaluation of Measurement Data—Guide to the Expression of Uncertainty in Measurement*; International Organization for Standardization: Geneva, Switzerland, 2008.
- [15] Overview of PEEK material, <http://www.matweb.com/> (visited on Dec. 2020)
- [16] Data on Al 1100, <http://www.matweb.com/> (visited on Dec. 2020)
- [17] L. Olivieri, A. Valmorbida, G. Sarego, E. Lungavia, D. Vertuani, E.C. Lorenzini, “Test of Tethered Deorbiting of Space Debris” *Advances in Astronautics Science and Technology*, 2020, 10.1007/s42423-020-00068-9
- [18] A. Valmorbida, M. Mazzucato, S. Tronco, M. Pertile, E.C. Lorenzini, “Design of a ground-based facility to reproduce satellite relative motions”, 2017 *IEEE MetroAeroSpace*, Padua (Italy), 2017, pp 468–473.
- [19] A. Valmorbida, M. Mazzucato, A. Aboudan, S. Tronco, “Test of attitude control maneuvers with a satellite formation lying testbed”, 2014 *IEEE MetroAeroSpace*, Benevento (Italy), 29–30 May 2014, pp 439–444.
- [20] A. Valmorbida, M. Mazzucato, S. Tronco, S. Debei, E.C. Lorenzini, “SPARTANS—a cooperating spacecraft testbed for autonomous proximity operations experiments”, *IEEE instrumentation and measurement technology conference*, vol 2015–July 2015.

A. Valmorbida, M. Mazzucato, M. Pertile, “Calibration procedures of a vision-based system for relative motion estimation between satellites flying in proximity”, *Measurement*, Volume 151, 2020, 107161, <https://doi.org/10.1016/j.measurement.2019.107161>